

Green Chemistry

Accepted Manuscript



This article can be cited before page numbers have been issued, to do this please use: A. Mohammadinezhad and B. Akhlaghnia, *Green Chem.*, 2017, DOI: 10.1039/C7GC02647A.



This is an Accepted Manuscript, which has been through the Royal Society of Chemistry peer review process and has been accepted for publication.

Accepted Manuscripts are published online shortly after acceptance, before technical editing, formatting and proof reading. Using this free service, authors can make their results available to the community, in citable form, before we publish the edited article. We will replace this Accepted Manuscript with the edited and formatted Advance Article as soon as it is available.

You can find more information about Accepted Manuscripts in the [author guidelines](#).

Please note that technical editing may introduce minor changes to the text and/or graphics, which may alter content. The journal's standard [Terms & Conditions](#) and the ethical guidelines, outlined in our [author and reviewer resource centre](#), still apply. In no event shall the Royal Society of Chemistry be held responsible for any errors or omissions in this Accepted Manuscript or any consequences arising from the use of any information it contains.



Journal Name

ARTICLE

Co^{II} immobilized on aminated Fe₃O₄@Boehmite nanoparticles (Fe₃O₄@Boehmite-NH₂-Co^{II} NPs): a novel, inexpensive and highly efficient heterogeneous magnetic nanocatalyst for Suzuki–Miyaura and Heck–Mizoroki cross-coupling reactions in green media

Received 00th January 20xx,
Accepted 00th January 20xx

DOI: 10.1039/x0xx00000x

www.rsc.org/

Arezou Mohammadinezhad^a, Batool Akhlaghinia^{a,*}

Herein we report the synthesis of a magnetically separable core-shell-like Fe₃O₄@Boehmite-NH₂-Co^{II} NPs as an environmentally friendly heterogeneous catalyst. The as-prepared nanocatalyst was well characterized by various techniques such as FT-IR, XRD, BET, TEM, FE-SEM, EDX, TGA, H₂-TPR, VSM, ICP-OES and elemental analysis and evaluated for the Suzuki–Miyaura and Heck–Mizoroki cross coupling reactions in green solvent (H₂O). The results of characterizations revealed the superparamagnetic behavior of the Fe₃O₄ NPs core encapsulated by a Boehmite NPs shell. Also, it was clearly found that the size of the particles was about 13–54 nm. In comparison to the previous reported catalysts, Fe₃O₄@Boehmite-NH₂-Co^{II} NPs exhibited perfect catalytic efficiency for the Suzuki–Miyaura and Heck–Mizoroki cross coupling reaction under mild conditions without using toxic solvents. The concerted effects between the individual components of catalyst and also its unique egg-like nanostructure caused the high catalytic performance of Fe₃O₄@Boehmite-NH₂-Co^{II} NPs. Also, the introduction of Co significantly lowers the cost of catalyst. More importantly, the longevity of nanocatalyst was studied and found that the magnetic nanocatalyst is stable under the reaction conditions and could be easily reused for at least seven consecutive cycles without a discernible decrease in its catalytic activity or metal leaching.

1. Introduction

Among the most fundamental reactions in organic chemistry, generating carbon–carbon bond as a powerful synthetic tool and a major area in multiple organic transformations has received great attention [1, 2] owing to, the resulting coupling products are widely used for academic and industrial process including pharmaceuticals, agrochemicals, natural products and fine chemical industries [3–6]. Undoubtedly, Suzuki–Miyaura [7] and Heck–Mizoroki [8] cross coupling reactions are the most beneficial and extensively used reactions for C–C bond formation due to their high efficiency and atom economy. In this context, novel transition metal complexes have been the most extensively studied catalytic systems for Suzuki–Miyaura [9] and Heck–Mizoroki [10] cross coupling reactions. During the last decades, Suzuki–Miyaura [11] and Heck–Mizoroki [12] coupling reactions were catalyzed by Pd based catalysts. More recently, in modern organic synthesis, considerable interest has been focused on palladium-free conditions and it has

been shown that transition metal catalysts, including nickel [13], copper [14], iron [15] and cobalt [16–18], might be employed as alternatives to toxic, air sensitive and expensive precious metal such as palladium in cross coupling reactions. Although, compared to nickel, palladium, and copper catalysts [19] coupling reaction under cobalt catalysis is rare [20, 21], but to date, cobalt catalysts have attracted substantial attention in organic synthesis owing to their higher reactivity for various C–C bond forming reactions, low cost, nontoxicity, availability and their interesting mode of action [22, 23]. There have been a number of important studies focused on the development of new catalytic systems and methodologies (including homogeneous and heterogeneous catalysts) based on cobalt in combination with different ligands to improve Suzuki–Miyaura and Heck–Mizoroki cross coupling reactions [16–18, 24–28].

For the past few years stabilized metallic nanoparticles (NPs) have probably been the most frequently employed in modern organic synthesis. Meanwhile, it has been demonstrated repeatedly that appropriate particle size, crystal structure and nature of ligand are crucial to access of metallic NPs with proper catalytic activity [29–31]. On the other hand, up to now magnetic nanocatalysts have attracted remarkable attention of organic chemists due to their feasible removal and recycling by means of an external magnetic field which is not time-consuming and prevents losing of catalyst during the separation process. Kinetic problems such as

^a Department of Chemistry, Faculty of Sciences, Ferdowsi University of Mashhad, Mashhad 9177948974, Iran.

† Footnotes relating to the title and/or authors should appear here.

Electronic Supplementary Information (ESI) available: [details of any supplementary information available should be included here]. See DOI: 10.1039/x0xx00000x

aggregation/ oxidation of metal particles and reduction in catalytic activity which are often caused by having very active surface atoms can be removed by a well-chosen stabilizer. The stabilizer can control the particle size, shape and magnetic features of the hybrid materials, improve the chemical stability, prevent the agglomeration and serve as the catalyst platform as well [32, 33].

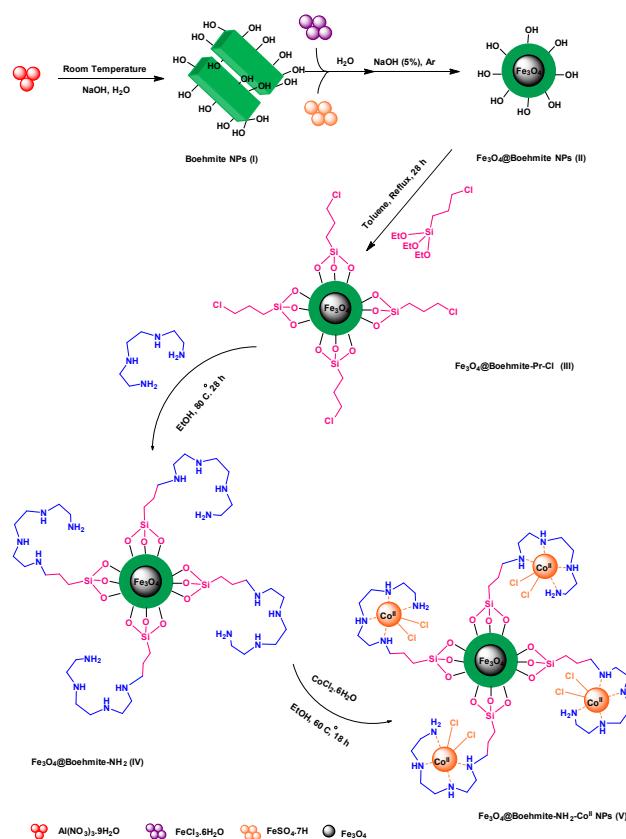
Boehmite NPs as a component of aluminium ore bauxite is an aluminum oxide hydroxide (γ -AlOOH) mineral. Boehmite NPs with orthorhombic unit cells consists of octahedral double sheets centered with aluminum ions. Extra hydroxyl groups on its surface provide the capability of reaction with different linkers and ligands which could be available for immobilization of metal ions [34]. Nontoxicity, availability, thermal and mechanical stability of Boehmite NPs makes it an excellent support, especially in heterogeneous catalysis [35-41]. With these considerations in mind, and to solve the problem of regeneration and reusing of the expensive catalyst, the use of Fe_3O_4 /Boehmite NPs hybrids is thus one of the most elegant and efficient way. As a part of our ongoing work towards the development of efficient green catalysts [42] we designed a novel procedure for the synthesis of Fe_3O_4 @Boehmite NPs with high magnetic feature and very small particle size compared to the previous reports in literature [43, 44]. In the following step, functionalization of Fe_3O_4 @Boehmite NPs was performed by the treatment with (3-choloropropyl)triethoxysilane and further reaction with triethylenetetramine to afford aminated Fe_3O_4 @Boehmite. With particular emphasis on the Suzuki–Miyaura and Heck–Mizoroki cross coupling reactions [43m, 43p] immobilization of Co^{II} were subsequently carried out *via* the reaction of Fe_3O_4 @Boehmite- NH_2 with ethanolic solution of $\text{CoCl}_2 \cdot 6\text{H}_2\text{O}$. A schematic illustration of the preparation strategy of the Co^{II} immobilized on aminated Fe_3O_4 @Boehmite nanoparticles (Fe_3O_4 @Boehmite- NH_2 - Co^{II} NPs) was shown in Scheme 1.

Results and Discussion

Characterization of Fe_3O_4 @Boehmite- NH_2 - Co^{II} NPs

The catalytic system was well characterized using various techniques including Fourier transform infrared spectroscopy (FT-IR), X-ray powder diffraction (XRD), Brunauer, Emmett and Teller (BET) surface area analysis, transmission electron microscopy (TEM), field emission scanning electron microscopy (FE-SEM), energy-dispersive X-ray (EDX), thermogravimetric analysis (TGA), hydrogen temperature-programmed reduction (H_2 -TPR), vibrating sample magnetometer (VSM), inductively coupled plasma optical emission spectroscopy (ICP-OES) and elemental analysis (CHN).

Fourier transform infrared (FT-IR) spectroscopy evidences the modification of Fe_3O_4 @Boehmite NPs surface. Fig. 1 demonstrates the FT-IR spectra of Boehmite NPs (a), Fe_3O_4 @Boehmite NPs (b), Fe_3O_4 @Boehmite-Pr-Cl (c), Fe_3O_4 @Boehmite- NH_2 (d), Fe_3O_4 @Boehmite- NH_2 - Co^{II} NPs (e) and 7th reused Fe_3O_4 @Boehmite- NH_2 - Co^{II} NPs (f). As shown in Fig. 1a, two strong absorption bands at 3294 and 3095 cm^{-1} correspond to both asymmetric and symmetric vibrational modes of the O-H bonds of Boehmite NPs. Three distinctive bands at 752, 630 and 522 cm^{-1} were attributed to Al-O vibrations. Existence of hydrogen bonded hydroxyl groups (OH...OH) was confirmed by the appearance of two absorption bands at 1154



Scheme 1. The magnetic nanocatalyst preparation.

and 1069 cm^{-1} . Fig. 1b displays a weak absorption band at 571 cm^{-1} related to the Fe-O bond of Fe_3O_4 @Boehmite NPs. Successful coupling of (3-choloropropyl)triethoxysilane to the surface of Fe_3O_4 @Boehmite NPs was demonstrated by the characteristic bending and stretching vibrations of the C-H and Si-O bonds which were appeared at 1292 and 1074 cm^{-1} respectively (Fig. 1c) [35, 39, 40, 45]. The existence of grafted TETA could be authenticated by the appearance of three new absorption bands at 2492, 1637 and 1447 cm^{-1} which can be assigned to N-H (primary and secondary amine) bending vibrations (Fig. 1d). Also, the stretching vibration band of N-H bond (3300-3000 cm^{-1}) could not be precisely defined, because of covering with the broad absorption band of OH...OH bond. Upon Co^{II} coordination, the intensity of the characteristic absorption band related to N-H bending vibration was decreased considerably (Fig. 1e) [46]. Moreover, the bands at 3555 and 1638 cm^{-1} were attributed to the O-H stretching of the lattice water molecule in the cobalt complex [47, 48].

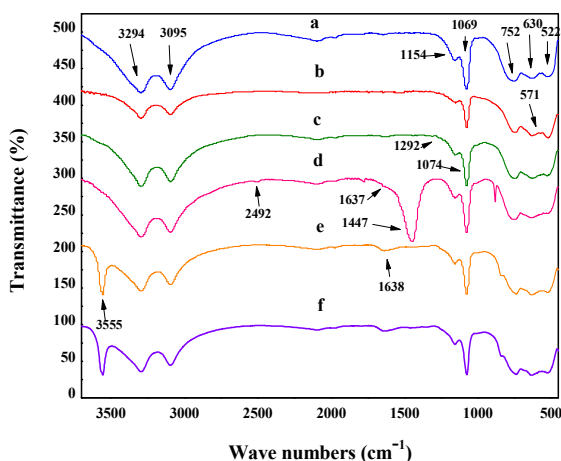


Fig. 1. FT-IR spectra of Boehmite NPs (a), Fe₃O₄@Boehmite NPs (b), Fe₃O₄@Boehmite-Pr-Cl (c), Fe₃O₄@Boehmite-NH₂ (d), Fe₃O₄@Boehmite-NH₂-Co^{II} NPs (e) and 7th reused Fe₃O₄@Boehmite-NH₂-Co^{II} NPs (f).

The crystallographic structures of Boehmite NPs (Fig. S1a), Fe₃O₄@Boehmite NPs (Fig. S1b) and Fe₃O₄@Boehmite-NH₂-Co^{II} NPs (Fig. S1c) were investigated by XRD technique. As shown in Fig. S1a, the Boehmite NPs phase was identified by the peak positions at $2\theta = 14.64$ (0 2 0), 28.36 (1 2 0), 38.50 (0 3 1), 46.01 (1 3 1), 49.41 (0 5 1), 51.79 (2 0 0), 55.41 (1 5 1), 60.76 (0 8 0), 64.15 (2 3 1), 65.14 (0 0 2), 67.86 (1 7 1), and 72.07 (2 5 1) which can be confirmed the crystallization of Boehmite NPs with an orthorhombic unit cell (Ref. Code: 98-004-6842). In Fig. S1b, the appearance of the characteristic peaks at $2\theta = 30.27$ (2 2 0), 35.74 (3 1 1), 43.27 (4 0 0), 53.78 (4 2 2), 57.29 (5 1 1) and 62.87 (4 4 0) are imputed to the cubic structure of Fe₃O₄ MNPs (Ref. Code: 98-007-7842). Similarly (in Fig. S1c), the crystalline peaks occurring at $2\theta = 14.87$ (0 2 0), 28.61 (1 2 0), 38.76 (0 3 1), 45.95 (1 3 1), 49.37 (0 5 1), 51.99 (2 0 0), 72.37 (2 5 1) and $2\theta = 30.6$ (2 2 0), 35.97 (3 1 1), 57.57 (5 1 1) are associated to the Boehmite NPs (Ref. Code: 98-000-6538) and Fe₃O₄ NPs (Ref. Code: 98-001-7260), respectively [35, 39, 49, 50]. The intensity of all peaks was decreased due to the chemical modifications. In comparison, the crystallinity value of the Fe₃O₄@Boehmite NPs and Fe₃O₄@Boehmite-NH₂-Co^{II} NPs was diminished because of deformation of hydrogen bonding in Boehmite NPs upon chemical modifications. Moreover, the X-ray diagram of the Fe₃O₄@Boehmite-NH₂-Co^{II} NPs showed four new peaks at $2\theta = 16.53$ (1 1 0), 32.14 (2 2 0), 54.09 (1 4 1) and 63.16 (5 0 3) which can be attributed to Co^{II} species (Fig. S1c) [51]. Besides, the average crystalline size of Fe₃O₄@Boehmite-NH₂-Co^{II} NPs which was calculated using Debye-Scherrer equation ($d = \lambda / (\beta \cos \theta)$) is estimated to be 33 nm (Fig. S1, Supplementary Material, page 3).

The nitrogen adsorption-desorption isotherm of Boehmite NPs (a), Fe₃O₄@Boehmite NPs (b) and Fe₃O₄@Boehmite-NH₂-Co^{II} NPs (c) are depicted in Fig. S2. As can be seen in Fig. S2, the appearance of H3-type hysteresis loops can be identified as type IV isotherm (based

on IUPAC classification) which is the characteristic of mesoporous materials. The specific surface area, pore volume and mean pore diameter of Boehmite NPs (a), Fe₃O₄@Boehmite NPs (b) and Fe₃O₄@Boehmite-NH₂-Co^{II} NPs (c) were shown in Table 1. Based on the Brunauer-Emmett-Teller (BET) analysis the average surface area of Boehmite NPs, Fe₃O₄@Boehmite NPs and Fe₃O₄@Boehmite-NH₂-Co^{II} NPs were 20, 46 and 34 m² g⁻¹, respectively. It is interesting to note that the low surface area of Boehmite NPs was attributed to the effect of NaOH:Al(NO₃)₃·9H₂O molar ratio and pH during the synthetic process [52, 53]. As can be concluded from Table 1, the increased in the BET surface area and decreased in the pore volume of Fe₃O₄@Boehmite NPs confirmed the entrance of Fe₃O₄ NPs into the Boehmite NPs pores. Likewise, owing to blocking of some pores by organic linkers upon functionalization process, the surface area of Fe₃O₄@Boehmite-NH₂-Co^{II} NPs was decreased. Also, the mean pore diameter and pore volume of Fe₃O₄@Boehmite NPs were increased after modification process, according to the data summarized in Table 1. These results clearly verify the well grafting of organic segments on the surface of Boehmite NPs (Fig. S2 and Table 1, Supplementary Material, page 4).

The size and morphology of the fresh Fe₃O₄@Boehmite-NH₂-Co^{II} NPs and 7th recovered Fe₃O₄@Boehmite-NH₂-Co^{II} NPs were studied by TEM technique. Typical TEM images and particle size distributions of core-shell Fe₃O₄@Boehmite-NH₂-Co^{II} NPs are shown in Figure S3 and S4. It was easily observed in Figure S3a, that the Fe₃O₄ NPs core is well encapsulated by a Boehmite NPs coating and a clear boundary between the Boehmite NPs shell and the Fe₃O₄ NPs core is observed in the egg-like nanostructure. As shown in Figure S3 (a and b) and Figure S4, the particle sizes of Fe₃O₄@Boehmite-NH₂-Co^{II} NPs in irregular geometric shape were about 13-54 nm (Fig. S3 and S4, Supplementary Material, page 5).

The size and morphology of Fe₃O₄@Boehmite-NH₂-Co^{II} NPs was also studied by field emission scanning electron microscopy (FE-SEM) technique. As can be seen in Fig. S5, the synthesized nanocatalyst showed good dispersity with an average size about 20-30 nm which is very close to the particle size as determined using TEM and XRD analysis (Fig. S5, Supplementary Material, page 6).

To survey the type of elements in Fe₃O₄@Boehmite-NH₂-Co^{II} NPs, the energy-dispersive X-ray (EDX) spectrum was taken and shown in Fig. S6. The composition of as-synthesized catalyst (Fe₃O₄@Boehmite-NH₂-Co^{II} NPs) was confirmed by the presence of O, Fe, Co, Al and Cl in the EDX spectrum (Fig. S6, Supplementary Material, page 6).

The thermogravimetric analysis (TGA) was used to determine the thermal stability and the amount of organic moieties on the surface of Fe₃O₄@Boehmite NPs. The TGA thermograms of Fe₃O₄@Boehmite NPs (a), Fe₃O₄@Boehmite-Pr-Cl (b), Fe₃O₄@Boehmite-NH₂-Co^{II} NPs (c) and 7th reused Fe₃O₄@Boehmite-NH₂-Co^{II} NPs (d) were shown in Fig. S7. As can be observed in Fig. S7a, the negligible weight loss (0.46%) from 20 to 100 °C was attributed to the removal of adsorbed and interstitial water [38]. Also, the observed weight loss (8.54%) at 410 to 600 °C corresponds to the transformation of γ -AlOOH into γ -Al₂O₃ [52]. The well crossbred of the organic spacer groups ((3-chloropropyl)triethoxysilane) on the surface of Fe₃O₄@Boehmite

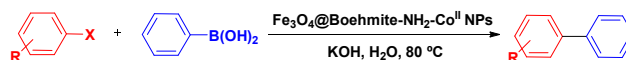
NPs were confirmed by the appearance of a new weight loss (9%) from 120 to 250 °C (Fig. S7b). In the profile of Fe₃O₄@Boehmite-NH₂-Co^{II} NPs, the TGA thermogram (Fig. S7c) depicted two-step thermal decomposition. The first step of weight loss (9%) from 120 to 250 °C was caused by the disintegration of the grafted (3-chloropropyl)triethoxysilane. The second weight loss (24%) from 250 to 600 °C is ascribed to the transformation of γ-ALOOH into γ-Al₂O₃ and also decomposition of the grafted triethylenetetramine. A good agreement was observed between the elemental analysis and TGA data, according to the results summarized in Table 2 (Table 2, Supplementary Material, page 7). These results clearly corroborated that organic functional groups incorporated on the surface of Fe₃O₄@Boehmite NPs (Fig. S7, Supplementary Material, page 7).

H₂-TPR was used to investigate the type of Co species on the surface of Fe₃O₄@Boehmite NPs. The TPR curves of Fe₃O₄@Boehmite-NH₂-Co^{II} NPs (a) and 7th reused Fe₃O₄@Boehmite-NH₂-Co^{II} NPs (b) were shown in Fig. S8. Two distinct reduction peaks were recognized. The first observed peak centered at 550 °C can be attributed to the reduction of immobilized Co^{II} to the metallic cobalt [54]. The second-step reduction peak may be assigned to the adsorbed cobalt species on the surface of Fe₃O₄@Boehmite NPs. Formation of cobalt aluminate due to strong interaction between Co^{II} and Al^{III} ions caused the reduction of surface Co^{II} at higher temperature (710 °C) [55, 56] (Fig. S8, Supplementary Material, page 8).

Magnetic properties of Fe₃O₄@Boehmite NPs and Fe₃O₄@Boehmite-NH₂-Co^{II} NPs were investigated by a vibrating sample magnetometer (VSM). As illustrated in Fig. S9, both samples are superparamagnetic nanoparticles. It can be seen that the saturation magnetization value of Fe₃O₄@Boehmite NPs and Fe₃O₄@Boehmite-NH₂-Co^{II} NPs were 37.52 and 25.1 emu g⁻¹, respectively. Compared with Fe₃O₄@Boehmite NPs, the saturation magnetization (MS) intensity of Fe₃O₄@Boehmite-NH₂-Co^{II} NPs was decreased drastically upon functionalization of Fe₃O₄@Boehmite NPs by organic segments. However, this magnetic property was high enough to provide easy and quick separation of the nanocatalyst from the reaction mixture with an external magnet (Fig. S9, Supplementary Material, page 8).

Catalytic performance of the Fe₃O₄@Boehmite-NH₂-Co^{II} NPs for the Suzuki–Miyaura and Heck–Mizoroki cross coupling reactions

Here, to evaluate the efficiency of the Fe₃O₄@Boehmite-NH₂-Co^{II} NPs catalyst system, the catalytic property of Fe₃O₄@Boehmite-NH₂-Co^{II} NPs was investigated in C–C bond formation *via* Suzuki–Miyaura cross coupling reaction (Scheme 2). Initially, the reaction between 4-iodobenzene and phenylboronic acid was chosen as a model reaction. To obtain the optimal conditions, the critical parameters to the outcome of the reaction such as solvent, base, temperature and catalyst loading were compared. The results of the optimization of conditions are summarized in Table 3 (Table 3, Supplementary Material, page 9).



R = H, 4-Cl, 4-NO₂, 4-Me, 4-OMe, 2Me-4-NO₂, 2-Thienyl, 3-CHO, 4-CHO, 4-CN, 4-NH₂, 2-NH₂

X = I, Br, Cl

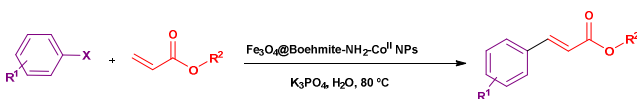
Scheme 2. Suzuki–Miyaura cross coupling reaction in the presence of Fe₃O₄@Boehmite-NH₂-Co^{II} NPs.

In our first set of experiments, a DMF solution of 4-iodobenzene (1mmol) was allowed to react with phenylboronic acid (1.2 mmol) in the presence of 0.33 mol% of Fe₃O₄@Boehmite-NH₂-Co^{II} NPs and 2 equivalents of K₂CO₃. Warming the reaction mixture to 100 °C, afforded the cross-coupling product with 65% yield after 60 min (Table 3, entry 1). To access the best optimal catalyst conditions, the effect of various solvents on the model reaction was investigated in-depth (Table 3, entries 2-10). The results of these experiments reveal that among the different solvents screened (DMSO, PEG, THF, *n*-hexane, toluene, 1,4-dioxane, CH₃CN, EtOH and H₂O), H₂O can be used as a green, inexpensive and efficient solvent for the Suzuki–Miyaura cross coupling reaction. The results of Table 3 confirmed that a basic environment was also crucial to the Suzuki–Miyaura cross coupling reaction (Table 3, entry 11). Several common bases were tested for the Suzuki–Miyaura cross coupling reaction in the presence of Fe₃O₄@Boehmite-NH₂-Co^{II} NPs (Table 3, entries 12-15). KOH afforded higher yield than the other bases. Then it was selected as the base for the subsequent experiments of the Suzuki–Miyaura cross coupling reaction. Not surprisingly, the results depended on the amount of the base used. After a few attempts, it was found that 3 equivalents of KOH were required to obtain the best yield of the corresponding product in short reaction time (Table 3, entries 15-17). It was found that temperature has an essential effect in this catalytic system, when the model reaction was carried out at different temperatures. As can be seen in Table 3, the most suitable temperature for Suzuki–Miyaura cross coupling reaction in the presence of Fe₃O₄@Boehmite-NH₂-Co^{II} NPs was 80 °C (Table 3, entries 18-21). Afterwards, the catalyst loading was also optimized by performing the model reaction in the presence of different amounts of catalyst. Higher yield of the desired product in short reaction time was afforded by employing 0.33 mol% of nanocatalyst. A significant decrease in the yield of reaction was observed by applying 0.22 mol% of catalyst, whereas additional amounts of catalyst (0.44 mol%) was not effective on the yield and rate of reaction significantly (Table 3, entries 22-23). To clarify the especial catalytic activity of Fe₃O₄@Boehmite-NH₂-Co^{II} NPs in Suzuki–Miyaura cross coupling reaction, in a set of experiments the model reaction was carried out in the absence of any catalyst and also in the presence of Fe₃O₄ NPs, Fe₃O₄@Boehmite NPs, Fe₃O₄@Boehmite-Pr-Cl, Fe₃O₄@Boehmite-NH₂ and CoCl₂·6H₂O respectively (Table 3, entries 24-29). All of cases were relatively insufficient for the coupling of 4-iodobenzene with phenylboronic acid as a benchmark reaction with observed conversion yields of 20%, 20%, 5%, 5%, 5% and 40% after 24 h, respectively (Table 3, Supplementary Material, page 9).

The generality of this nanoparticles Co^{II} catalyst was investigated on the substrate scope for Suzuki–Miyaura cross coupling reaction.

Under the optimized reaction conditions (Table 3, Supplementary Material, page 9, entry 19), a variety of structurally divergent aryl iodides, bromides, and chlorides reacted with phenylboronic acid to generate the desired coupling products (Table 4). The coupling reactions of aryl iodides and aryl bromides took place in short period of time with good to high yields whereas aryl chlorides due to the low reactivity of C–Cl bond cannot produce the satisfactory yields of coupling products even after prolonged reaction times (compare entries 1–18 with 19–23). Although aryl bromides required longer times to afford the same result as aryl iodides (compare entries 1–9 with 10–18)). This might be due to the leaving group ability of halogens ($\text{I} > \text{Br} > \text{Cl} > \text{F}$). In the present catalytic system, the electronic and steric effects on the yields and reaction rates were also studied. This catalytic system showed a good efficiency with a range of both electron-rich and electron-poor substituted aryl halides (such as 4- $\text{NO}_2\text{C}_6\text{H}_4$, 4- ClC_6H_4 , 4- OMeC_6H_4 , 4- MeC_6H_4 , 4- CNC_6H_4 , 3- CHOC_6H_4 , 4- CHOC_6H_4 , 4- $\text{NH}_2\text{C}_6\text{H}_4$ and 2- $\text{NH}_2\text{C}_6\text{H}_4$). Electron-withdrawing groups accelerated the Suzuki–Miyaura cross coupling reaction and exhibited better conversions as well, in comparison with the electron-donating substituents (compare entries 2,3 with 4,5,8,9 and entries 11, 12, 13 with 16, 17, 18 and 21 with 22, 23). It was observed that the *ortho* substituted aryl halides afforded the corresponding products with acceptable yield in longer reaction time than those obtained with *para*-substituted ones reflecting steric effects (Table 4, compare entries 6, 9, 18, 23 with 8, 17, 22).

In addition to improving conditions for the Suzuki–Miyaura cross coupling reaction, the possibility of performing Heck–Mizoroki cross coupling reaction in the presence of $\text{Fe}_3\text{O}_4@$ Boehmite- NH_2 - Co^{II} NPs was strategically explored (Scheme 3).

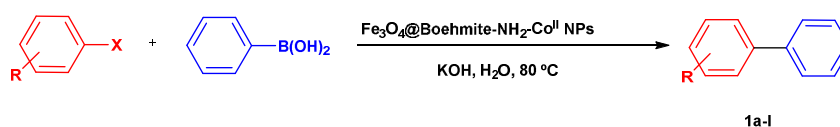


$\text{R}^1 = \text{H}, 4\text{-NO}_2, 4\text{-Cl}, 4\text{-OMe}, 4\text{-Me}, 4\text{-CN}, 4\text{-CHO}, 2\text{-Thienyl}, 4\text{-NH}_2, 2\text{-NH}_2$

$\text{X} = \text{I}, \text{Br}, \text{Cl}$

$\text{R}^2 = \text{Me}, \text{Bu}^n$

Table 4. Suzuki–Miyaura cross-coupling reactions of different aryl halides with phenylboronic acid catalyzed by $\text{Fe}_3\text{O}_4@$ Boehmite- NH_2 - Co^{II} NPs.



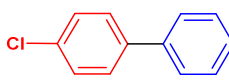
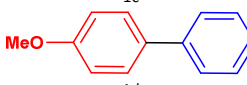
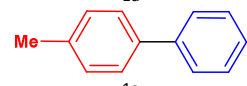
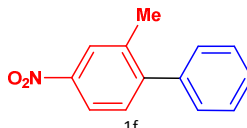
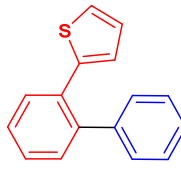
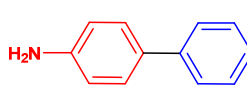
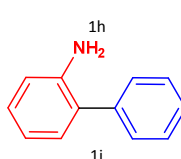
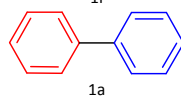
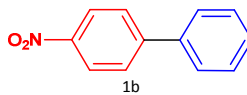
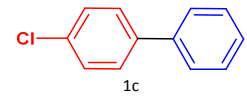
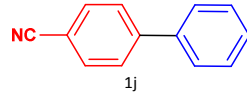
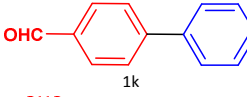
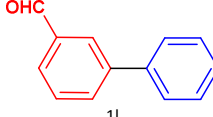
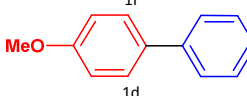
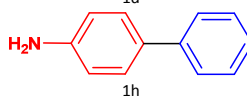
Entry	R	X	Product	Time (min)	Isolated Yield (%)
1	H	I	1a	30	95
2	4- NO_2	I	1b	25	95

Scheme 3. Heck–Mizoroki cross coupling reaction in the presence of $\text{Fe}_3\text{O}_4@$ Boehmite- NH_2 - Co^{II} NPs

To test the feasibility of Co^{II} -catalyzed Heck–Mizoroki cross coupling reaction, 4-iodobenzene (1 mmol) and methyl acrylate (1.2 mmol) were used as the benchmark substrates. For this purpose, reaction conditions such as solvent, base, reaction temperature and catalyst quantity were optimized (Table 5). In surveying of common solvents (DMF, DMSO, PEG, THF, *n*-hexane, toluene, 1,4-dioxane, CH_3CN , EtOH and H_2O), it was found that only poor yields were obtained with solvents such as THF, *n*-hexane, toluene, 1,4-dioxane and CH_3CN while the yield and reaction rate was enhanced in DMF, DMSO, PEG, EtOH and H_2O (Table 5, entries 1–10). Considering economic and environmental factors H_2O was chosen as the best solvent for the Heck–Mizoroki cross coupling reaction in the presence of $\text{Fe}_3\text{O}_4@$ Boehmite- NH_2 - Co^{II} NPs. We further turned our attention to study the effect of base in the Heck–Mizoroki cross coupling reaction. Our studies revealed that K_3PO_4 was optimal. Lower yields were provided with Li_2CO_3 , NaHCO_3 and KOH (Table 5, entries 11–14). As can be seen in Table 5, the role of base is mainly in the Heck–Mizoroki cross coupling reaction and the desired product was obtained in highest yield by applying 1/4 molar ratio of 4-iodobenzene / K_3PO_4 (Table 5, entries 15–18). Further optimization was examined on the effect of temperature and catalyst loading (Table 5, entries 19–25). The finding suggests that the yield and reaction rate were enhanced drastically (95% in 45 min) in the presence of 0.44 mol% of $\text{Fe}_3\text{O}_4@$ Boehmite- NH_2 - Co^{II} NPs at 80 °C. To demonstrate the efficiency catalytic activity of $\text{Fe}_3\text{O}_4@$ Boehmite- NH_2 - Co^{II} NPs in the Heck–Mizoroki cross coupling reaction, the model reaction was performed without using catalyst. After long period of time, poor yield of product was gained as well as in the presence of Fe_3O NPs, $\text{Fe}_3\text{O}_4@$ Boehmite NPs, $\text{Fe}_3\text{O}_4@$ Boehmite-Pr-Cl, $\text{Fe}_3\text{O}_4@$ Boehmite- NH_2 and $\text{CoCl}_2 \cdot 6\text{H}_2\text{O}$ respectively (Table 5, entries 26–30) (Table 5, Supplementary Material, page 11).

ARTICLE

Journal Name

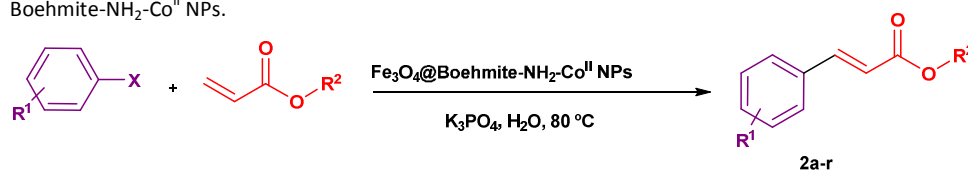
3	4-Cl	I	 1c	25	93
4	4-OMe	I	 1d	70	93
5	4-Me	I	 1e	65	95
6	2-Me-4-NO ₂	I	 1f	50	90
7	2-Thienyl	I	 1g	90	85
8	4-NH ₂	I	 1h	2 (h)	98
9	2-NH ₂	I	 1i	3 (h)	60
10	H	Br	 1a	35	95
11	4-NO ₂	Br	 1b	40	95
12	4-Cl	Br	 1c	40	90
13	4-CN	Br	 1j	35	93
14	4-CHO	Br	 1k	75	95
15	3-CHO	Br	 1l	90	95
16	4-OMe	Br	 1d	160	85
17	4-NH ₂	Br	 1h	3 (h)	90

18	2-NH ₂	Br		4 (h)	50
			1i		
19	H	Cl		3 (h)	45
			1a		
20	4-CHO	Cl		4 (h)	50
			1k		
21	4-CN	Cl		2 (h)	65
			1j		
22	4-NH ₂	Cl		7 (h)	20
			1h		
23	2-NH ₂	Cl		9 (h)	15
			1i		

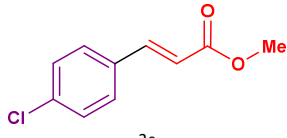
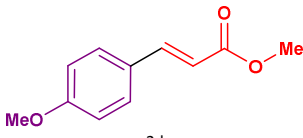
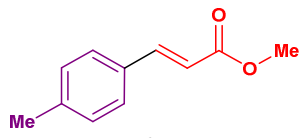
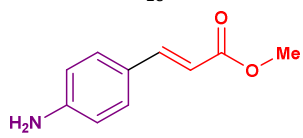
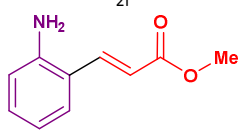
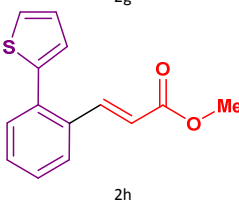
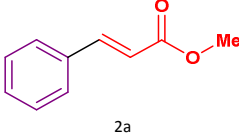
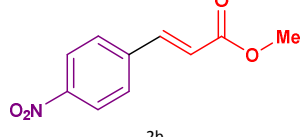
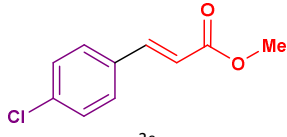
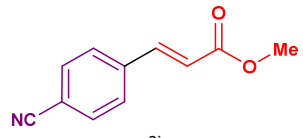
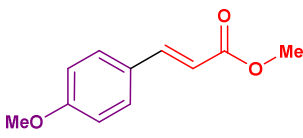
Subsequently, to explore the scope and generality of the present method in the Heck–Mizoroki cross coupling reaction, the optimized reaction conditions were applied for the reaction of a wide variety of aryl halides including electron-donating and electron-withdrawing groups on the aromatic ring with various olefins. The results of this study are summarized in Table 6. By analyzing Table 6, it was found that all reactions of different substituted aryl iodides with methyl acrylate / or *n*-butyl acrylate generated products with yields considered high in short reaction time (Table 6, entries 1-8 and entries 20-25). Notably aryl iodides with electron-withdrawing substituents react with olefins more quickly than those with electron-donating substituents. But as

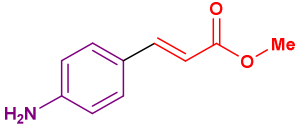
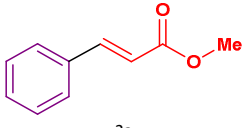
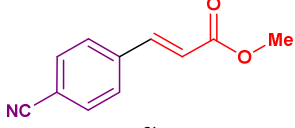
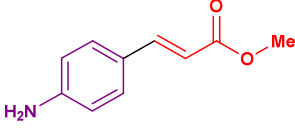
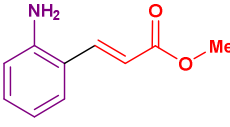
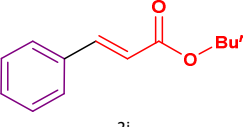
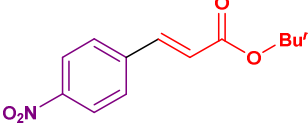
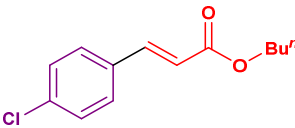
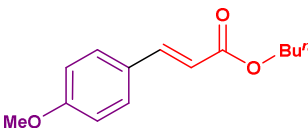
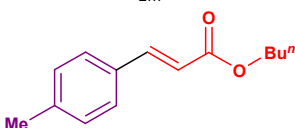
expected the reactivity of C-halogen bond have influence that interfere with the reaction, the coupling reaction appears sluggish with aryl bromides, gives lower yield under optimized conditions (compare entries 1-8 with entries 9-15). The present strategy can be further extended to the coupling reaction of aryl chlorides with methyl acrylate / or *n*-butyl acrylate under similar catalytic conditions. Table 6 obviously reveals that the Heck–Mizoroki cross coupling reaction of aryl chloride in the presence of Fe₃O₄@Boehmite-NH₂-Co^{II} NPs leads to unusually less product yield even after long period of time (Table 6, entries 16-19 and entries 29-32).

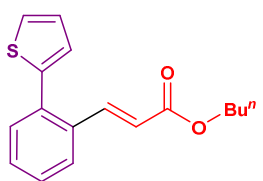
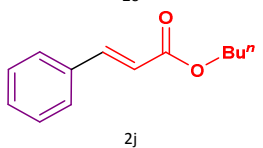
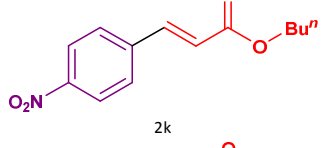
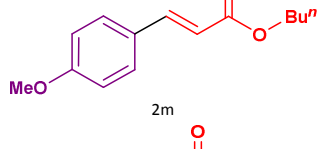
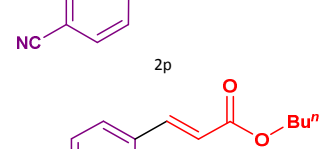
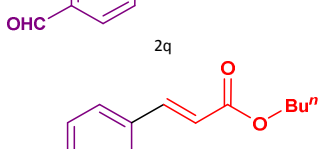
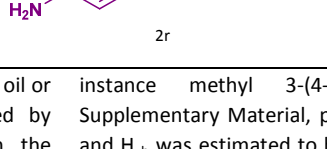
Table 6. Heck–Mizoroki cross cross-coupling reactions of different aryl halides with olefins catalyzed by Fe₃O₄@Boehmite-NH₂-Co^{II} NPs.



Entry	R ¹	R ²	X	Product	Time (min)	Isolated Yield (%)
1	H	Me	I	2a	45	95
2	4-NO ₂	Me	I	2b	25	95

3	4-Cl	Me	I		35	92
4	4-OMe	Me	I		60	80
5	4-Me	Me	I		55	85
6	4-NH ₂	Me	I		2 (h)	98
7	2-NH ₂	Me	I		3 (h)	25
8	2-Thienyl	Me	I		85	75
9	H	Me	Br		100	85
10	4-NO ₂	Me	Br		90	90
11	4-Cl	Me	Br		90	87
12	4-CN	Me	Br		70	90
13	4-OMe	Me	Br		3 (h)	75

14	4-NH ₂	Me	Br		4 (h)	70
15	2-NH ₂	Me	Br		5 (h)	40
16	H	Me	Cl		4 (h)	25
17	4-CN	Me	Cl		3 (h)	40
18	4-NH ₂	Me	Cl		6 (h)	25
19	2-NH ₂	Me	Cl		7 (h)	15
20	H	Bu ⁿ	I		30	95
21	4-NO ₂	Bu ⁿ	I		30	95
22	4-Cl	Bu ⁿ	I		30	90
23	4-OMe	Bu ⁿ	I		40	85
24	4-Me	Bu ⁿ	I		40	88

25	2-Thienyl	Bu ⁿ	I		70	80
26	H	Bu ⁿ	Br		95	85
27	4-NO ₂	Bu ⁿ	Br		95	85
28	4-OMe	Bu ⁿ	Br		2 (h)	77
29	H	Bu ⁿ	Cl		3 (h)	30
30	4-CN	Bu ⁿ	Cl		3 (h)	35
31	4-CHO	Bu ⁿ	Cl		5 (h)	30
32	4-NH ₂	Bu ⁿ	Cl		7 (h)	15

All of the synthesized compounds were known and isolated as oil or solid products. The obtained products were characterized by comparing their melting points with those reported in the literature. Molecular ion peaks of all prepared products exhibited their respective *m/e*, according to the mass spectrometric data. In addition, the structure of the selected compounds was further investigated by surveying their high-field ¹H NMR, ¹³C NMR and FT-IR spectral data. The disappearance of starting materials confirmed the completion of the reaction which was monitored by TLC.

Based on the ¹H NMR spectral data (Fig. 1-22, Supplementary Material, page 15-55), Fe₃O₄@Boehmite-NH₂-Co^{II} NPs catalyzed the Heck–Mizoroki cross coupling reaction in a stereospecific manner and in all of the reactions E-isomers were produced predominately. By considering the ¹H NMR spectrum of product in details for

instance methyl 3-(4-chlorophenyl) acrylate (Fig. S10, Supplementary Material, page 13), the coupling constant (*J*) of H_a and H_b was estimated to be ~ 18 Hz, which is the characteristic of trans isomers.

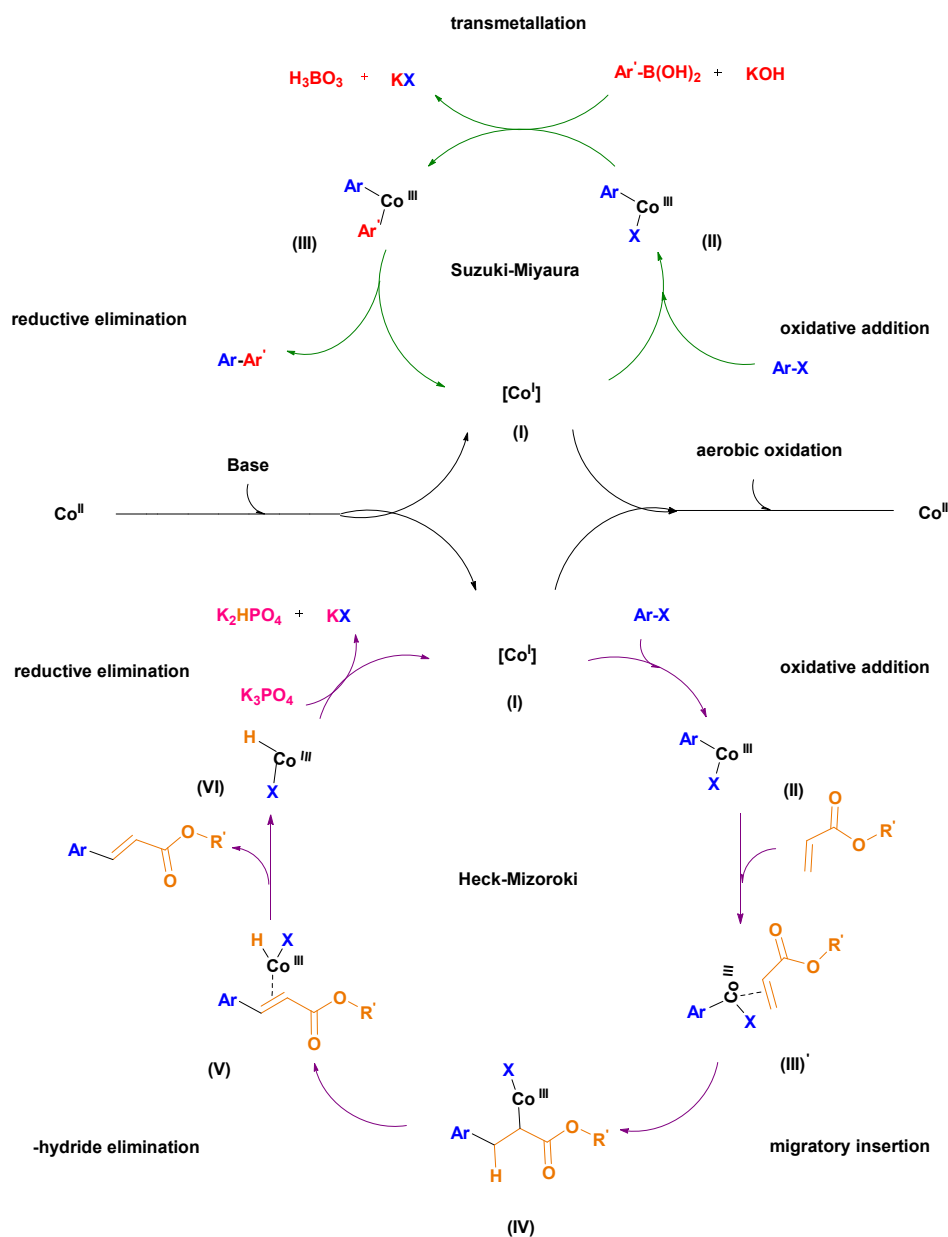
In analogy with the previous reports [57-59] and based on our findings a plausible mechanism for the Suzuki–Miyaura and Heck–Mizoroki cross coupling reactions is proposed in scheme 4. At the beginning, the reaction was thought to be initiated by an *in situ* reduction of Co^{II} complexes to Co^I or Co⁰ species (I) in the presence of KOH/ K₃PO₄ [60] (To probe whether Co^I or Co⁰ species fulfilled the cross coupling reactions, we performed the model reactions in the presence of CoBr and Co(0)). The coupling products were produced with satisfactory yields in the presence of CoBr whereas under the same reaction conditions, no significant yields were observed in the

presence of Co^0 . This finding suggests that the reactions proceeds *via* the formation of the active Co^I species).

Then, upon the oxidative addition of aryl halide to low valent Co^I , aryl cobalt intermediate (II) was afforded. In the following step, transmetalation of (II) with arylboronic acid in the presence of KOH afforded $\text{Ar-Co}^III\text{-Ar}'$ intermediate (III). Finally, reductive elimination produced the biaryl product and regenerated the Co^I species (I). Completion of the catalytic cycle for the Suzuki–Miyaura cross coupling reaction was achieved by aerobic oxidation of the Co^I species (I) to the Co^{II} complexes [61].

In our working suggestion for the Heck–Mizoroki cross coupling reaction, it was expected that low valent Co^I species (I) can be added to an olefin to afford adduct (IV) *via* the formation of (III') (upon olefin coordination). Following β -hydride elimination, a

new olefin and hydridocobalt (VI) was produced. Finally, a reductive elimination regenerated the active Co^I species (I) in the presence of K_3PO_4 . Subsequent aerobic oxidation furnished Co^{II} complexes [61].



Scheme 4. Proposed mechanism for the Suzuki–Miyaura and Heck–Mizoroki cross coupling reactions in the presence of Fe₃O₄@Boehmite-NH₂-Co^{II} NPs.

From the green chemistry viewpoint, reusability is one of the most important properties of metal catalysis that should be studied. In this regard, the reusability of Fe₃O₄@Boehmite-NH₂-Co^{II} NPs was studied by consecutive the Heck–Mizoroki cross coupling reaction of 4-iodobenzene with methyl acrylate under the optimized reaction conditions. After the first catalytic cycle, the nanocatalyst was easily separated by means of an external magnetic field from the reaction mixture, washed with ethanol and acetone (3 × 5 mL) and dried at 50 °C overnight. Then a new coupling reaction of fresh reactants was started using the recovered catalyst. The catalyst was stable and reusable for up to 7 runs during the catalytic reaction as it afforded almost identical results in each cycle and slightly decrease in the yields was observed in 6th and 7th cycles (Table 7). The turn over frequency (TOF) and turn over number (TON) of the catalyst were also calculated and the results are shown in Table 7. As can be seen the supreme catalytic activity of Fe₃O₄@Boehmite-NH₂-Co^{II} NPs was not significantly decrease even after 7 recycle runs.

Table 7. Reusability of Fe₃O₄@Boehmite-NH₂-Co^{II} NPs in the Heck–Mizoroki reaction of 4-iodobenzene with methyl acrylate under the optimized reaction conditions.

Entry	Time (min)	Isolated Yield (%)	TOF (h ⁻¹)	TON
1	45	95	2.87	2.15
2	45	95	2.87	2.15
3	45	95	2.87	2.15
4 ^a	45/50	91/95	2.74/2.58	2.06/2.15
5 ^a	45/53	90/95	2.72/2.43	2.04/2.15
6 ^a	45/55	88/95	2.66/2.34	2/2.15
7 ^a	45/60	85/95	2.57/2.15	1.93/2.15

^aThe second numbers in the second columns correspond to the isolated yield after 50, 53, 55 and 60 min.

To elucidate the long-term durability of the catalyst as an important issue, after seven cycles in the Heck–Mizoroki cross coupling reaction, any structural changes of Fe₃O₄@Boehmite-NH₂-Co^{II} NPs was investigated by FT-IR, XRD, TEM, TGA, H₂-TPR and ICP-OES techniques. It is clearly evident from the FT-IR spectrum of the 7th reused Fe₃O₄@Boehmite-NH₂-Co^{II} NPs that the metallic ions were strongly bounded to the surface of Fe₃O₄@Boehmite NPs through the coordination of the organic segments and also, no important changes in the frequencies, intensities and shapes of absorption bands were observed (Fig. 1f).

Interestingly, comparing the XRD pattern of fresh and 7th reused Fe₃O₄@Boehmite-NH₂-Co^{II} NPs exhibited that no significant broadening or shifting was happened in the characteristic diffraction peaks (Fig. S1d, Supplementary Material, page 3).

The TEM images of the 7th recovered Fe₃O₄@Boehmite-NH₂-Co^{II} NPs were shown in Fig. S3 (c and d) (Fig. S3, Supplementary Material, page 5). Interestingly, no agglomeration or increase in the particle size was observed even after 7 consecutive recycle runs.

Furthermore, by comparing the TGA thermogram of the fresh Fe₃O₄@Boehmite-NH₂-Co^{II} NPs with the 7th recovered nanocatalyst, it could be concluded that no significant differences were observed in the decomposition pattern (compare Fig. S7c with S7d, Supplementary Material, page 7). However, the weight loss of the grafted organic motif was decreased from 33% (in the fresh nanocatalyst) to 32% in the 7th recycled nanocatalyst. Accordingly, the amount of the grafted (3-choloropropyl)triethoxysilane was decreased from 1.16 to 1.03 mmol g⁻¹ after 7 cycles, which might be ascribed to the diminutive leaching of organic segments during recycling process.

As can be inferred from H₂-TPR of the 7th recovered Fe₃O₄@Boehmite-NH₂-Co^{II} NPs (Fig. S8b, Supplementary Material, page 8), the oxidation state of Co was not changed even after 7 recycle runs.

In order to quantitative analysis and realize the exact amount of cobalt in the fresh and reused Fe₃O₄@Boehmite-NH₂-Co^{II} NPs, ICP-OES technique has been applied in the model Heck–Mizoroki cross coupling reaction. The ICP-OES analysis showed that 1.1 and 1.04 mmol of cobalt were anchored on 1.000 g of the fresh and 7th reused nanocatalyst, respectively. According to the obtained data, no significant leaching of cobalt from the surface of Fe₃O₄@Boehmite-NH₂-Co^{II} NPs was observed.

The obtained results from FT-IR, XRD, TEM, TGA and H₂-TPR undoubtedly confirmed that the physical properties of Fe₃O₄@Boehmite-NH₂-Co^{II} NPs including functional groups, crystallographic structure, shape, morphology, particle size, thermal stability and oxidation sate were preserved in the reaction media even after 7 recycle runs.

Heterogeneity studies

In the present study, to investigate the homogeneity/heterogeneity nature of the catalyst, we introduced the hot filtration test, kinetic study and three-phase test. In the following, all of them were discussed in details.

Hot filtration test

A hot filtration test was performed to find out whether Fe₃O₄@Boehmite-NH₂-Co^{II} NPs acts as a heterogeneous catalyst or solely serves as a Co^{II} ion source by leaching out into the solution to form the active catalyst species. Toward this point, the Suzuki–Miyaura and Heck–Mizoroki cross coupling reactions were studied under the optimal conditions. In half time of the Suzuki–Miyaura /and Heck–Mizoroki cross coupling reaction of 4-iodobenzene with phenylboronic acid/ and methyl acrylate, the catalyst was separated using an external magnetic field and the reaction was then permitted to continue without catalyst for further 2/ and 3 h. The reaction progress was followed by thin layer chromatography.

There was no further coupling reaction, even after an extended time, indicated that a negligible amount of active species (less than 0.31 mol% according to the ICP-OES analysis) leached out during the catalytic reaction. The results established the strong attachment of cobalt nanoparticles to the Fe_3O_4 @Boehmite NPs surface. It is worth to mention that although a positive hot-filtration test highlights the homogeneity of the catalyst, but a negative test does not allude to the heterogeneous nature of the catalyst due to the quickly re-deposition of soluble active species. Therefore, to assess the homogeneity/heterogeneity of the catalyst further experiments are required [50].

Kinetic study

In order to further explore the possibility of the heterogeneous nature of Fe_3O_4 @Boehmite- NH_2 - Co^{II} NPs, a kinetic study was performed. To this end, two different parameters (reaction yield and cobalt leaching) were investigated on the model Heck-Mizoroki cross coupling reaction under the optimized reaction condition. To determine the cobalt concentration in solution, 4 samples of the reaction mixture were taken during the reaction. In each case, the samples were analyzed by ICP-OES as well as the yield of the reaction was monitored by GC. The results were described in Fig. S11. No obvious leaching was observed, according to the ICP-OES data (Fig. S11b). In the other word, the cobalt concentration in solution is presumably very small (0.000084, 0.000088, 0.000096 and 0.000096 mol % after 15, 30, 45 and 60 min, respectively). It could be found that a negligible amount of cobalt in solution had not a considerable effect on the reaction progress and a notable increase in the reaction yield could be attributed to the heterogenous cobalt species. According to the obtained results, the conclusion could be derived that the heterogenous cobalt species are the catalyst promoter in this reaction (Fig. S11, Supplementary Material, page 13).

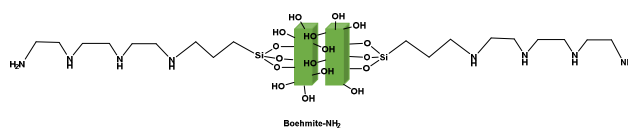
Three-phase test

Table 8. Comparison of the catalytic activity of Fe_3O_4 @Boehmite- NH_2 - Co^{II} NPs with literature precedents using Ni, Fe and Co based heterogeneous catalysts for the Heck–Mizoroki cross coupling reaction.

Entry	Catalyst	Solvent	Temperature (°C)	Time (h)	Yield (%)	Reference
1	Ni(II)-DABCO@ SiO_2	DMF	100	3	97	10
2	SiO_2 -Fe(acac)	PEG	130	1.5	85	15
3	Co hollow nanospheres	NMP	130	16	73	24
4	Nano Co	NMP	140	16	85	25
5	Co/ Al_2O_3	NMP	150	24	56	28
6	Co-NHC@MWCNTs ^a	PEG	80	5	85	27
7	Co-IL@MWCNTs ^b	Toluene	100	3	87	26
8	Co-MS@MNPs/CS ^c	PEG	80	1	88	62
9	Nano Co	NMP	120	8	90	63
10	Fe_3O_4 @Boehmite- NH_2 - Co^{II} NPs	H_2O	80	45 (min)	95	Present study

^a Multi walled carbon nanotubes supported N-heterocyclic carbene–cobalt (II).

To gain insight into the nature of the nanocatalyst, a three-phase test was designed. Three-phase test is a powerful technique that allows the catalyst to be in its nature habitat. To conduct the test, the model Heck-Mizoroki cross coupling reaction was carried out in the absence and in the presence of Boehmite- NH_2 NPs (Scheme 5) as a strong scavenger to capture the homogeneous soluble cobalt ions. The reaction progress was monitored by GC. The results are depicted in Fig. S12. As it is evident in Fig. S12b, the presence of scavenger has no effect on the yield of the reaction. According to the above observation, it could be concluded that there is no soluble cobalt ions in solution and the reaction arguably proceeds in a heterogeneous pathway. All of the results obtained from heterogeneity tests confirmed that the Fe_3O_4 @Boehmite- NH_2 - Co^{II} NPs had a high catalytic activity with a truly stable heterogeneous nature under the described reaction conditions (Fig. S12, Supplementary Material, page 14).



Scheme 5. Boehmite- NH_2 NPs.

To attain further evaluation of the efficiency of Fe_3O_4 @Boehmite- NH_2 - Co^{II} NPs, we compared the catalytic activity of the catalyst with some of the previously reported heterogeneous (Ni, Fe and Co) catalysts in the Heck–Mizoroki cross coupling reaction (Table 8). Although all of the listed catalysts can produce the desired product in good to excellent yield, but it can be clearly found that Fe_3O_4 @Boehmite- NH_2 - Co^{II} NPs is superior to most of the well-known supported catalyst systems in terms of reaction conditions (solvent (entries 1-9), temperature (entries 1-5 and entries 7 and 9), reaction time (entries 1-7 and 9), recovery and reusability (entries 1-7 and 9) as well as price and toxicity.

^b Cobalt nanoparticles supported on ionic liquid-functionalized multiwall carbon nanotubes.^c Cobalt immobilized on MNPs-chitosan functionalized with methyl salicylate (Co-MS@MNPs/CS).

Conclusion

In the present study Fe_3O_4 @Boehmite- NH_2 - Co^{II} NPs was synthesized and characterized as an environmentally-friendly nanocatalyst for the Suzuki–Miyaura and Heck–Mizoroki cross coupling reactions with various electronically diverse substrates. The experimental results displayed the core-shell structure of the synthesized catalyst with a mean size range of 13–54 nm. Owing to the cooperative interaction of the four dentate triethylenetetramine anchored on aminated Fe_3O_4 @Boehmite, the nanocatalyst presented high cobalt content with negligible metal leaching during the course of reaction. Subsequently, high yields in short reaction times were achieved without the need for an expensive palladium catalyst as well as excellent reusability for at least seven times in the corresponding reaction without a reduction in catalytic activity. Notably, the superior catalytic activity of using Fe_3O_4 @Boehmite- NH_2 - Co^{II} NPs in C–C bond formation was characterized by using a chemically stable and magnetic recyclable nanocatalyst (which can replace Pd, Ni and Fe complexes for the Suzuki–Miyaura and Heck–Mizoroki cross coupling reactions), using a benign solvent system without the need for any special conditions and minimal Co usage. The use of this new catalyst in organic synthesis will be extended in our laboratory.

Experimental

General

The purity determinations of the products and the progress of the reactions were accomplished by TLC on silica gel polygram STL G/UV 254 plates (preparative TLC was carried out using a Merck GF 254 silica gel on a glass support) or column chromatography on silica gel 60 (230–400 mesh) and GC-17A Shimadzu device. The melting points of products were determined with an Electrothermal Type 9100 melting point apparatus. The FT-IR spectra were recorded on an Avatar 370 FT-IR Thermo Nicolet spectrometer. The NMR spectra were provided on Bruker Avance 300, 400 and 500 MHz instruments in CDCl_3 . Elemental analysis was performed using a Thermo Finnigan Flash EA 1112 Series instrument. Mass spectra were recorded with a CH7A Varianmat Bremem instrument at 70 eV electron impact ionization, in m/z (rel %). X-ray powder diffraction (XRD) was performed on a PANalytical Company X'Pert Pro MPD diffractometer with Cu K α radiation ($\lambda = 0.154$ nm) radiation. BET surface area and pore size distribution were measured on a Belsorp mini II system at -196 °C using N_2 as the adsorbate. Transmission electron microscopy (TEM) was performed with a Leo 912 AB (120 kV) microscope (Zeiss, Germany). FE-SEM images were recorded using a TESCAN, Model: MIRA3 scanning electron microscope operating at an acceleration voltage of 30.0 kV (manufactured by the Czech Republic). Elemental compositions were determined with an SC7620 energy-dispersive X-ray analysis (EDX) presenting a 133 eV resolution at 20 kV. Thermogravimetric analyses (TGA and DTG) were carried out using a Shimadzu Thermogravimetric Analyzer (TG-50) in the temperature range of 25–950 °C at a heating rate of 10 °C min^{-1} , under air atmosphere. Hydrogen temperature-

programmed reduction (H_2 -TPR) was carried out using a Quantachrome ChemBET 3000. The magnetic property of catalyst was measured using a vibrating sample magnetometer (VSM, Magnetic Danesh Pajoh Inst). Inductively coupled plasma optical emission spectroscopy (ICP-OES) was carried out on a 76004555 SPECTRO ARCOS ICP-OES analyzer. All yields refer to isolated products after purification by thin layer chromatography/ or column chromatography.

Preparation of the Boehmite NPs (I)

To a solutions of NaOH (162 mmol, 6.490 g) in 50 mL distilled water, a solution of $\text{Al}(\text{NO}_3)_3 \cdot 9\text{H}_2\text{O}$ (53 mmol, 20 g) in distilled water (30 mL) was added drop wise by the rate of 2.94 mL/min under vigorous stirring. After 18 min the resulting milky mixture was subjected to mixing in ultrasonic bath for 3 h at 25 °C. The obtained Boehmite NPs (I) was filtered and washed by distilled water and was kept in the oven at 220 °C for 4 h [64].

Preparation of Fe_3O_4 @Boehmite NPs (II)

Boehmite NPs (I) (2 g) was dispersed in 100 mL of deionized water for 30 min. Then, $\text{FeCl}_3 \cdot 6\text{H}_2\text{O}$ (11.5 mmol, 3.1 g) and $\text{FeSO}_4 \cdot 7\text{H}_2\text{O}$ (7.5 mmol, 2.1 g) were added to the white suspension. The resulting mixture was mechanically stirred for 3 min at room temperature under Ar atmosphere. Afterwards, 50 mL NaOH (5%) was added very slowly into the mixture under vigorous stirring. The resulting black mixture was continuously stirred for 2 h at 90 °C under Ar atmosphere. Finally, the mixture was permitted to cool to room temperature and then Fe_3O_4 @Boehmite NPs (II) was separated by an external magnet and washed with deionized water several times before dried at 50 °C overnight.

Preparation of Fe_3O_4 @Boehmite-Pr-Cl (III)

Fe_3O_4 @Boehmite NPs (II) (1.5 g) was dispersed in dry toluene (50 mL) for 30 min. Thereafter, (3-chloropropyl)triethoxysilane (2.5 mmol, 0.6 g) was added to the resulting suspension. The mixture was refluxed for 28 h. Then, the obtained Fe_3O_4 @Boehmite-Pr-Cl (III) was filtered, washed with ethanol (5 \times 10 mL) and dried at 50 °C overnight [40].

Preparation of Fe_3O_4 @Boehmite- NH_2 (IV)

To a suspension of Fe_3O_4 @Boehmite-Pr-Cl (III) (1 g) in 50 mL ethanol, triethylenetetramine (2.5 mmol, 0.365 g) was added at room temperature. The resulting mixture was stirred at 80 °C for 28 h. Then, Fe_3O_4 @Boehmite- NH_2 (IV) was filtered, washed with ethanol (5 \times 10 mL) and dried at 50 °C overnight.

Preparation of Fe_3O_4 @Boehmite- NH_2 - Co^{II} NPs (V)

To a solution of $\text{CoCl}_2 \cdot 6\text{H}_2\text{O}$ (4.2 mmol, 0.99 g) in absolute EtOH (5 mL), Fe_3O_4 @Boehmite- NH_2 (IV) (1 g) was added and stirred at 60 °C for 18 h. The resulting Fe_3O_4 @Boehmite- NH_2 - Co^{II} NPs (V) was then filtered, washed with ethanol (3 \times 10 mL) to remove the unreacted materials, and finally dried at 50 °C overnight.

Typical procedure for Suzuki–Miyaura cross coupling reaction

Potassium hydroxide (3 mmol, 0.168 g) was added to a mixture of 4-iodobenzene (1.0 mmol, 0.203 g) and phenylboronic acid (1.2

mmol, 0.146 g) in water (3 mL) at 80 °C. Then, Fe₃O₄@Boehmite-NH₂-Co^{II} NPs (V) (0.33 mol%, 0.003g) was added to the resulting mixture under stirring. After the completion of the reaction (30 min) which was monitored by TLC, the nanocatalyst was separated by a magnetic field, washed with ethyl acetate and dried at room temperature for 24 h for the next run use. The reaction mixture was then extracted with ethyl acetate (5 × 5 mL) and the combined organic layer was dried over anhydrous Na₂SO₄. After evaporation of the solvent, the crude product was purified by thin layer chromatography (or column chromatography using *n*-hexane/ethylacetate (8 : 2) solvent mixture) using *n*-hexane/ethyl acetate (50/1) to afford the pure 1,1'-biphenyl (0.145 g, % 95 yield).

Typical procedure for Heck–Mizoroki cross coupling reaction

To a mixture of K₃PO₄ (4 mmol, 0.849 g), methyl acrylate (1.2 mmol, 0.108 mL), and 4-iodobenzene (1.0 mmol, 0.203 g) in H₂O (3 mL) Fe₃O₄@Boehmite-NH₂-Co^{II} NPs (V) (0.44 mol%, 0.004 g) was added at room temperature. The resulting mixture was heated at 80 °C in an oil bath. After the completion of the reaction (45 min) which was monitored by TLC, the nanocatalyst was separated by a magnetic field, washed with ethyl acetate and dried at room temperature for 24 h for the next run use. The reaction mixture was then extracted with ethyl acetate (5 × 5 mL) and the combined organic layer was dried over anhydrous Na₂SO₄. After evaporation of the solvent, the crude product was purified by thin layer chromatography (or column chromatography using *n*-hexane/ethylacetate (8 : 2) solvent mixture) using *n*-hexane/ethyl acetate (50/1) to afford the pure methyl cinnamate (0.153 g, % 95 yield).

Acknowledgements

The authors gratefully acknowledge the partial support of this study by Ferdowsi University of Mashhad Research Council (Grant no. p/3/43367).

References

- [1] A. M. Thomas, A. Sujatha and G. Anilkumar, *RSC Adv.*, 2014, **4**, 21688–21698.
- [2] F. Yang, S. Y. Fu, W. Chu, C. Li and D. G. Tong, *RSC Adv.*, 2014, **4**, 45838–45843.
- [3] J. G. de Vries, *Can. J. Chem.*, 2001, **79**, 1086–1092.
- [4] F. Leroux, *Chem. Bio. Chem.*, 2004, **5**, 644–649.
- [5] S. Lightowler and M. Hird, *Chem. Mater.*, 2005, **17**, 5538–5549.
- [6] M. C. Kozłowski, B. J. Morgan and E. C. Linton., *Chem. Soc. Rev.*, 2009, **38**, 3193–3207.
- [7] G. Yue, Y. Wu, C. Wu, Z. Yin, H. Chen, X. Wang and Z. Zhang, *Tetrahedron Lett.*, 2017, **58**, 666–669.
- [8] A. B. Dounay and L. E. Overman, *Chem. Rev.* 2003, **103**, 2945–2963.
- [9] C. Wang, L. Salmon, R. Ciganda, L. Yates, S. Moya, d J. Ruiz and D. Astruc, *Chem. Commun.*, 2017, **53**, 644–646.
- [10] A. R. Hajipour and P. Abolfathi, *Catal. Lett.*, 2017, **147**, 188–195.
- [11] Y. Wang, C. Lu, G. Yang, Z. Chen and J. Nie, *React. Funct. Polym.*, 2017, **110**, 38–46.
- [12] N. Khadir, G. Tavakoli, A. Assoud, M. Bagherzadeh and D. M. Boghaei, *Inorganica. Chimica. Acta.*, 2016, **440**, 107–117.
- [13] S. Ma, H. Wang, K. Gao and F. Zhao, *J. Mol. Catal. A: Chem.*, 2006, **248**, 17–20.
- [14] S. G. Babu, N. Neelakandeswari, N. Dharmaraj, S. D. Jackson and R. Karvembu, *RSC Adv.*, 2013, **3**, 7774–7781.
- [15] A. R. Hajipour and G. Azizi, *Green Chem.*, 2013, **15**, 1030–1034.
- [16] Y. Ikeda, T. Nakamura, H. Yorimitsu and K. Oshima, *J. Am. Chem. Soc.*, 2002, **124**, 6514–6515.
- [17] C. Gosmini, J. M. B'egouin and A. Moncomble, *Chem. Commun.*, 2008, **0**, 3221–3233.
- [18] W. Lixia, W. Zi-wei, W. Guosong, L. Xiaodong and R. Jianguo, *Polym. Adv. Technol.*, 2010, **21**, 244–249.
- [19] B. M. Trost, I. Fleming, C. H. Heathcock, *Comprehensive Ve Organic Synthesis*, Pergamon Press: New York, 1991.
- [20] (a) G. Cahiez and H. Avedissian, *Tetrahedron Lett.*, 1998, **39**, 6159–6162; (b) H. Avedissian, L. Be'rilion, G. Cahiez and P. Knochel, *Tetrahedron Lett.*, 1998, **39**, 6163–6166. (c) Y. Nishii, K. Wakasugi and Y. Tanabe, *Synlett*, 1998, **1**, 67–69.
- [21] T. Kauffmann, *Angew. Chem., Int. Ed. Engl.*, 1996, **35**, 386–403.
- [22] C. S. Guo, C. M. Weng and F. E. Hong, *Eur. J. Inorg. Chem.*, 2010, **2010**, 3220–3228.
- [23] J. M. Hammann, D. Haas and P. Knochel, *Angew. Chem. Int. Ed.*, 2015, **54**, 4478–4481.
- [24] P. Zhou, Y. Li, P. Sun, J. Zhou and J. Bao, *Chem. Commun.*, 2007, **0**, 1418–1420.
- [25] H. Qi, W. Zhang, X. Wang, H. Li, J. Chen, K. Peng and M. Shao, *Catal. Commun.*, 2009, **10**, 1178–1183.
- [26] A. R. Hajipour, Z. Khorsandi and H. Karimi, *Appl. Organometal. Chem.*, 2015, **29**, 805–808.
- [27] A. R. Hajipour and Z. Khorsandi, *Catal. Commun.*, 2016, **77**, 1–4.
- [28] S. Iyer and V. V. Thakur, *J. Mol. Catal. A: Chem.*, 2000, **157**, 275–278.
- [29] V. G. Ramu, A. Bordoloi, T. C. Nagaiah, W. Schuhmann, M. Muhler and C. Cabrele, *Appl. Catal. A.*, 2012, **88**, 431–432.
- [30] O. V. Kharissova, B. I. Kharisov, V. M. Jimenez-Perez, B. Munoz Flores and U. Ortiz Mendez, *RSC Adv.*, 2013, **3**, 22648–22682.
- [31] A. Pal, I. Sevonkaev, B. Bartling, J. Rijssenbeek and D. V. Goia, *RSC Adv.*, 2014, **4**, 20909–20914.
- [32] (a) L. Levy, Y. Sahoo, K. S. Kim, E. J. Bergey and P. N. Prasad, *Chem. Mater.*, 2002, **14**, 3715–3721; (b) S. Sacanna, L. Rossi and A. P. Phillipse, *Langmuir*, 2007, **23**, 9974–9982; (c) A. Xia, J. Hu, C. Wang and D. Jiang, *Small*, 2007, **3**, 1811–1817.
- [33] F. Nador, M. A. Volpe, F. Alonso, A. Feldhoff, A. Kirschning and G. Radivoy, *Appl. Catal., A*, 2013, **455**, 39–45.
- [34] V. Vatanpour, S. S. Madaenia, L. Rajabi, S. Zinadini and A. A. Derakhshan, *J. Membr. Sci.*, 2012, **401**, 132–143.

ARTICLE

Journal Name

- [35] K. Bahrami, M. M. Khodaei and M. Roostaei, *New J. Chem.*, 2014, **38**, 5515-5520.
- [36] E. Carbonell, E. Delgado-Pinar, J. Pitarch-Jarque, J. Alarcón and E. García-Españ, *J. Phys. Chem.*, 2013, **117**, 14325-14331.
- [37] M. Hajjami, A. Ghorbani-Choghamarani, R. Ghafouri-Nejad and B. Tahmasbi, *New J. Chem.*, 2016, **40**, 3066-3074.
- [38] A. Ghorbani-Choghamarani, P. Moradi and B. Tahmasbi, *RSC Adv.*, 2016, **6**, 56638-56646.
- [39] A. Ghorbani-Choghamarani, P. Moradi and B. Tahmasbi, *RSC Adv.*, 2016, **6**, 43205-43216.
- [40] B. Tahmasbi and A. Ghorbani-Choghamarani, *Catal. Lett.*, 2017, **147**, 649-662.
- [41] A. Ghorbani-Choghamarani, M. Hajjami, B. Tahmasbi and N. Noori, *J. Iran Chem. Soc.*, 2016, **13**, 2193-2202.
- [42] (a) N. Razavi and B. Akhlaghinia, *RSC Adv.*, 2015, **5**, 12372-12381; (b) S. S. E. Ghodsinia and B. Akhlaghinia, *RSC Adv.*, 2015, **5**, 49849-49860; (c) M. Zarghani and B. Akhlaghinia, *Appl. Organomet. Chem.*, 2015, **29**, 683-689; (d) Z. Zarei and B. Akhlaghinia, *Chem. Pap.*, 2015, **69**, 1421-1437; (e) M. Zarghani and B. Akhlaghinia, *RSC Adv.*, 2015, **5**, 87769-87780; (f) N. Razavi and B. Akhlaghinia, *New J. Chem.*, 2016, **40**, 447-457; (g) R. Jahanshahi and B. Akhlaghinia, *RSC Adv.*, 2015, **5**, 104087-104094; (h) N. Yousefi Siavashi, B. Akhlaghinia and M. Zarghani, *Res. Chem. Intermed.*, 2016, **42**, 5789-5806; (i) E. Karimian, B. Akhlaghinia and S. S. E. Ghodsinia, *J. Chem. Sci.*, 2016, **128**, 429-439; (j) R. Jahanshahi and B. Akhlaghinia, *RSC Adv.*, 2016, **6**, 29210-29219; (k) M. Zarghani and B. Akhlaghinia, *RSC Adv.*, 2016, **6**, 31850-31860; (l) S. S. E. Ghodsinia, B. Akhlaghinia and R. Jahanshahi, *RSC Adv.*, 2016, **6**, 63613-63623; (m) M. Zarghani and B. Akhlaghinia, *Bull. Chem. Soc. Jpn.*, 2016, **89**, 1192-1200; (n) S. M. Masjed, B. Akhlaghinia, M. Zarghani and N. Razavi, *Aust. J. Chem.*, 2017, **70**, 33-43; (o) Z. Zarei and B. Akhlaghinia, *RSC Adv.*, 2016, **6**, 106473-106484; (p) N. Razavi, B. Akhlaghinia and R. Jahanshahi, *Catal. Lett.*, 2017, **147**, 360-373; (q) R. Jahanshahi and B. Akhlaghinia, *Chem. Pap.*, 2017, **71**, 1351-1364; (r) M. Esmailpour, B. Akhlaghinia and R. Jahanshahi, *J. Chem. Sci.*, 2017, **129**, 313-328; (s) N. Mohammadian and B. Akhlaghinia, *Res. Chem. Intermed.*, 2017, **43**, 3325-3347; (t) M. Zarghani and B. Akhlaghinia, *RSC Advances*, 2016, **6**, 38592-38601; (u) R. Jahanshahi and B. Akhlaghinia, *New J. Chem.*, 2017, **41**, 7203-7219; (v) M. S. Ghasemzadeh and B. Akhlaghinia, *Bull. Chem. Soc. Jpn.*, 2017, **90**, 1119-1128; (w) A. Mohammadinezhad and B. Akhlaghinia, *Aust. J. Chem.*, 2017, DOI: 10.1071/CH17093; (x) R. Jahanshahi and B. Akhlaghinia, *Catal. Lett.*, 2017, **147**, 2640-2655; (y) M. Nejatianfar, B. Akhlaghinia and R. Jahanshahi, *Appl. Organomet. Chem.*, 2017, in press; (z) N. Mohammadian and B. Akhlaghinia, *Res. Chem. Intermed.*, 2017, DOI: 10.1007/s11164-017-3153-7.
- [43] Y. X. Zhang, X. Y. Yu, Z. Jin, Y. Jia, W. H. Xu, T. Luo, B. J. Zhu, J. H. Liu and X. J. Huang, *J. Mater. Chem.*, 2011, **21**, 16550-16557.
- [44] Y. Wei, R. Yang, Y. X. Zhang, L. Wang, J. H. Liu and X. J. Huang, *Chem. Commun.*, 2011, **47**, 11062-11064.
- [45] A. Ghorbani-Choghamarani and B. Tahmasbi, *New J. Chem.*, 2016, **40**, 1205-1212.
- [46] L. You, H. Jiang, X. Dong and C. Ma, *Int. J. Electrochem. Sci.*, 2017, **12**, 1680-1689.
- [47] D. Buckingham and D. Jones, *Inorg. Chem.*, 1965, **4**, 1387-1392.
- [48] M. E. Mahmouda, M. S. Abdelwahab and E. M. Fathallah, *Chem. Eng. J.*, 2013, **223**, 318-327.
- [49] B. Li, X. Wang, Y. Guo, A. Iqbal, Y. Dong, W. Li, W. Liu, W. Qin, S. Chen, X. Zhou and Y. Yang, *Dalton Trans.*, 2016, **45**, 5484-5491.
- [50] H. Huang, L. Wang, Y. Cai, C. Zhou, Y. Yuan, X. Zhang, H. Wan and G. Guan, *Cryst. Eng. Comm.*, 2014, **17**, 1318-1325.
- [51] J. Mizuno, *J. Phys. Soc. Jpn.*, 1960, **15**, 1412-1420.
- [52] T. E. Bell, J. M. González-Carballo, R. P. Tooze and L. Torrente-Murciano, *J. Mater. Chem. A*, 2015, **3**, 6196-6201.
- [53] Q. Yang, *Inorg. Mater.*, 2010, **46**, 953-958.
- [54] M. P. Rosynek and C. A. Polansky, *Appl. Catal., A*, 1991, **73**, 97-12.
- [55] Y. Liu, H. Guo, L. Jia, Z. Ma, Y. Xiao, C. Chen, M. Xia, B. Hou and D. Li, *J. Chem. Eng. Mater. Sci.*, 2014, **2**, 19-27.
- [56] G. S. Sewell, E. van Steen and C. T. O'Connor, *Catal. Lett.*, 1996, **37**, 255-260.
- [57] W. Affo, H. Ohmiya, T. Fujioka, Y. Ikeda, T. Nakamura, H. Yorimitsu, K. Oshima, Y. Imamura, T. Mizuta and K. Miyoshi, *J. AM. Chem. Soc.* 2006, **128**, 8068-8077.
- [58] S. Maity, P. Dolui, R. Kancherla and D. Maiti, *Chem. Sci.*, 2017, **8**, 5181-5185.
- [59] M. E. Weiss, L. M. Kreis, A. Lauber and E. M. Carreira, *Angew. Chem. Int. Ed.*, 2011, **50**, 11125-11128.
- [60] G. P. Cerai and B. Morandi, *Chem. Commun.*, 2016, **52**, 9769-9772.
- [61] E. Vinck, D. M. Murphy, I. A. Fallis, R. R. Strevens and S. V. Doorslaer, *Inorg. Chem.*, 2010, **49**, 2083-2092.
- [62] A. R. Hajipour, F. Rezaei and Z. Khorsandi, *Green Chem.*, 2017, **19**, 1353-1361.
- [63] K. S. Jithendra Kumara, G. Krishnamurthy, B. E. K. Swamy, N. S. Kumar and M. Kumar, *J. Porous Mater.*, 2017, **24**, 1095-1103.
- [64] L. Rajabi and A. Derakhshan, *Sci. Adv. Mater.*, 2010, **2**, 163-172.